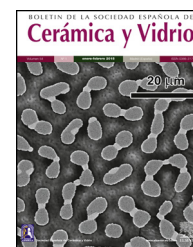




BOLETIN DE LA SOCIEDAD ESPAÑOLA DE

# Cerámica y Vidrio

[www.elsevier.es/bsecv](http://www.elsevier.es/bsecv)


## Original article

# Effect of Mo content on the properties of graphite–MoC composites sintered by spark plasma sintering

Marta Suárez<sup>a</sup>, Daniel Fernández-González<sup>a,\*</sup>, Luis Antonio Díaz<sup>a</sup>,  
 Juan Piñuela-Noval<sup>a</sup>, Amparo Borrell<sup>b</sup>, José Serafín Moya<sup>a</sup>, Ramón Torrecillas<sup>a</sup>,  
 Adolfo Fernández<sup>a</sup>

<sup>a</sup> Nanomaterials and Nanotechnology Research Center (CINN-CSIC), Universidad de Oviedo (UO), Principado de Asturias (PA), El Entrego, Spain

<sup>b</sup> Instituto de Tecnología de Materiales, Universitat Politècnica de València (UPV), Valencia, Spain

### ARTICLE INFO

#### Article history:

Received 15 July 2022

Accepted 20 February 2023

Available online xxx

#### Keywords:

Graphite

Spark plasma sintering

Thermal conductivity

Mechanical properties

Electrical conductivity

### ABSTRACT

Graphite–molybdenum–titanium powders prepared by colloidal processing technique were sintered by Spark Plasma Sintering (SPS). This material is proposed in this manuscript due to its potential interest as heat sink. The influence of the molybdenum content (2.5, 5.0 and 10.0 vol.%) on the thermal, electrical, and mechanical properties of the composite are studied to define the composite with the best properties. Thermal, electrical, and mechanical properties of the composite graphite–10 vol.% Mo–1 vol.% Ti (that are composites of graphite with molybdenum and titanium carbides after sintering) are significantly better than those of the composites with lower molybdenum contents (2.5 vol.% and 5 vol.%). This way, flexural strength, electrical conductivity, and thermal conductivity are 1.5, 7.8 and 18 times greater, respectively, than in the composite graphite–2.5 vol.% Mo–1 vol.% Ti. In the case of comparing with the composite graphite–5 vol.% Mo–1 vol.% Ti, flexural strength, electrical conductivity, and thermal conductivity are 1.2, 5.1 and 3.2 greater in the composite graphite–10 vol.% Mo–1 vol.% Ti, respectively.

© 2023 The Author(s). Published by Elsevier España, S.L.U. on behalf of SECV. This is an open access article under the CC BY-NC-ND license (<http://creativecommons.org/licenses/by-nc-nd/4.0/>).

## Influencia del contenido en Mo en las propiedades de materiales compuestos de grafito–MoC sinterizados por Spark Plasma Sintering

### RESUMEN

Se sinterizaron por Spark Plasma Sintering (SPA) polvos de grafito–molibdeno–titanio preparados mediante la técnica de síntesis coloidal. En el presente manuscrito se propone este material debido a su potencial en disipadores de calor. Se estudió la influencia del contenido en molibdeno (2,5, 5,0 y 10,0 vol.%) en las propiedades térmicas, eléctricas y

#### Palabras clave:

Grafito

Spark plasma sintering

Conductividad térmica

\* Corresponding author.

E-mail address: [d.fernandez@cinn.es](mailto:d.fernandez@cinn.es) (D. Fernández-González).

<https://doi.org/10.1016/j.bsecv.2023.02.005>

0366-3175/© 2023 The Author(s). Published by Elsevier España, S.L.U. on behalf of SECV. This is an open access article under the CC BY-NC-ND license (<http://creativecommons.org/licenses/by-nc-nd/4.0/>).

Propiedades mecánicas  
Conductividad eléctrica

mecánicas del material compuesto para definir aquel con las mejores propiedades. De este modo, las propiedades térmicas, eléctricas y mecánicas del material compuesto grafito-10 vol.% Mo-1 vol.% Ti (que son composites de grafito con carburos de titanio y molibdeno tras la sinterización) son significativamente mejores que aquellas de los materiales compuestos con menores contenidos en molibdeno (2,5 vol.% y 5 vol.%). Así pues, la resistencia a flexión, la conductividad eléctrica y la conductividad térmica son 1,5, 7,8 y 18 veces superiores, respectivamente, a las del composite grafito-2,5 vol. Mo-1 vol.% Ti. Si la comparación se lleva a cabo con el material compuesto grafito-5 vol.% Mo-1 vol.% Ti, la resistencia a flexión, la conductividad eléctrica y la conductividad térmica son 1,2, 5,1 y 3,2 veces superiores en el material compuesto grafito-10 vol. Mo-1 vol.% Ti, respectivamente.

© 2023 El Autor(s). Publicado por Elsevier España, S.L.U. en nombre de SECV. Este es un artículo Open Access bajo la licencia CC BY-NC-ND (<http://creativecommons.org/licenses/by-nc-nd/4.0/>).

## Introduction

Graphite is a carbon allotrope characterized by the good thermal and electrical conductivities, which make it interesting for thermal management applications when it is adequately sintered. Nevertheless, thermal, electrical, and mechanical properties are sometimes poor for such applications and, metallic second phases are added to obtain graphite-metal composites with improved properties. These metallic second phases include molybdenum [1–4], aluminum [5–8], or copper [9–16]. Graphite-metal composites, and in particular graphite–molybdenum composites, have been subject of research for years [1]. Focusing on the case of graphite–molybdenum carbide composites, the interest mainly arises from the thermal-mechanical properties conferred by the molybdenum carbides (MoC and Mo<sub>2</sub>C). Within this line, White and Pontelandolfo produced graphite–molybdenum carbide composites by liquid phase sintering at high temperatures under applied pressure [17–19]. In addition, Harada and Rubin [20] studied the formation of carbides in graphite–molybdenum composites by hot pressing of petroleum coke (used as graphite source) and metal or metal carbide mixtures (prepared by dry blending of powders) at high temperatures (2000 °C). The excellent thermal, electrical, and mechanical properties of this composite, even under extreme conditions, have made them to find application in rocket nozzles [21] and, more recently, in collimators of particle accelerators for the Large Hadron Collider at CERN (Conseil Européen pour la Recherche Nucléaire) [22–24]. Within this last application, several researchers have proposed different methods to obtain the graphite–molybdenum carbide composites:

- Mariani [22] was involved in the preparation of molybdenum carbide-graphite composites by rapid hot pressing (10 min) at high temperatures (1700 °C). The process required the application of constant pressure (45 MPa) under vacuum (10<sup>-4</sup> mbar) and reducing atmosphere (97% N<sub>2</sub>–3% H<sub>2</sub>).
- Bertarelli and Bizarro [23] were also involved in the preparation of molybdenum carbide-ceramic composites by powder mixing, green compaction (10–20 MPa) and hot pressing at temperatures within 2500 and 2600 °C and pressures between 35 and 45 MPa.

- Guardia-Valenzuela and colleagues [24] prepared graphite–molybdenum carbide-titanium carbide composites from graphite, molybdenum (with a constant molybdenum content, 4.5 vol.%), titanium and, in some cases, carbon fibers. Powder mixture was prepared in a 3D mixing machine and, then powders were compacted by uniaxial hydraulic pressing at 300 MPa and sintered by spark plasma sintering at temperatures exceeding 2500 °C.

Graphite–molybdenum carbide composites have also potential application in the field of catalyzers for energy conversion devices. Within this line, Huang and colleagues synthesized graphite–Mo<sub>2</sub>C nanocomposites by solid-state reaction from melamine and MoO<sub>3</sub> as precursors under inert atmosphere. Then, pressed pellets of precursors were treated in a tubular furnace under N<sub>2</sub> flow at 1400 °C for 3 h [25].

Finally, our research group has also been involved in the research within the topic of graphite–molybdenum carbide composites for thermal management applications. We have investigated the utilization of colloidal synthesis and spark plasma sintering in the consolidation of graphite–molybdenum carbide–titanium carbide composite [26], which resulted in improved properties (thermal, electrical, and mechanical) with respect to those of the composite obtained by attrition milling and spark plasma sintering. This research reported that sintering at significantly lower temperature (2000 °C) than that indicated in Valenzuela et al. [24] (2600 °C) and, therefore, without involving liquid phase [27], was possible. Despite all the existing research within this topic, studies about the influence of molybdenum content on the graphite–molybdenum carbide composites were not found in the state of the art. Thus, the aim of the present manuscript is to study the influence of the molybdenum content on the final properties of graphite–molybdenum carbide-titanium carbide composites prepared by colloidal route and sintered by spark plasma sintering.

## Materials and methods

Graphite–molybdenum–titanium composite powders were prepared by colloidal processing route. Graphite powder (crystalline natural graphite, grade 93004, Asbury Carbons

Company, flake morphology,  $d_{50}=6.007\ \mu\text{m}$ , BET:  $17\ \text{m}^2/\text{g}$ ) was the matrix constituent of the composite and, molybdenum (V) chloride (Sigma–Aldrich, Spain) and titanium isopropoxide (ABCR, Spain) were the precursors of molybdenum and titanium, respectively, which were the disperse constituents.

Colloidal processing consisted in adding dropwise a solution of  $\text{MoCl}_5$  and  $\text{Ti}[\text{OCH}(\text{CH}_3)_2]_4$  in ethanol into the graphite dispersion also in ethanol. Then, the slurry was first heated under magnetic stirring at  $70^\circ\text{C}$  to facilitate the dispersion of the constituents and, it was later dried in drying oven under air atmosphere at  $120^\circ\text{C}$  for 24 h to start the nucleation of molybdenum and titanium and to evaporate the alcohol. Afterward, dried material was grounded, and the powder was sieved through  $<180\ \mu\text{m}$ . Finally, powders were subjected to heat treatment at  $450^\circ\text{C}$  for 2 h in air to eliminate chloride and isopropoxide traces and, powder was later sieved through  $<180\ \mu\text{m}$  before being sintered in the spark plasma sintering apparatus.

Green compacts of 40 mm in diameter and 3 mm in height were first obtained by uniaxial pressing at 15 MPa. These green compacts were later sintered in spark plasma sintering equipment (FCT-HP D25/1) using a graphite mold of 40 mm in diameter. Sintering cycle consisted in heating at a rate of  $25^\circ\text{C}\ \text{min}^{-1}$  up to  $1500^\circ\text{C}$  and  $10^\circ\text{C}\ \text{min}^{-1}$  to the final dwell temperature ( $2400^\circ\text{C}$ ) under an applied pressure of 30 MPa during all sintering process and vacuum conditions ( $10^{-1}$  mbar). Dwell time was 15 min, and cooling was carried out inside of the SPS equipment. Temperature was controlled by an axial pyrometer focused on the upper graphite punch measuring the temperature above the sample center, as it is the usual practice in this equipment.

Three molybdenum contents were chosen to evaluate their influence on the thermal, electrical, and mechanical properties of the composite on five specimens of each composition: 2.5 vol.%, 5 vol.% and 10 vol.% Mo. Titanium content was 1 vol.% in all the samples to stabilize at room temperature the cubic MoC formed at high temperatures. These three molybdenum contents were chosen to study a great field of compositions and optimize the number of experiments.

### Characterization techniques

Different techniques were employed to analyze the thermal, electrical, and mechanical properties as well as the microstructural characteristics of the composite. This way, the adequate distribution of the molybdenum and titanium nanoparticles chemically adhered to the graphite surface was corroborated by means of high-resolution transmission electron microscopy (HRTEM, JEOL JEM 2100F with an acceleration voltage of 200 kV and field emission gun). Powders of the composite were dispersed in ethanol and one droplet of dispersion was put on the carbon-copper grid for HRTEM observation.

The mineralogical phases of the powder and sintered samples were analyzed by X-ray diffraction (XRD) technique. A Philips X' Pert Pro X-ray diffractometer was used:  $\text{Cu-K}\alpha$  radiation ( $\lambda=0.15406\ \text{nm}$ ) in the range from  $5^\circ$  to  $70^\circ$ , with step size of  $0.030^\circ$  and step time 0.5 s. Peak fitting of the crystalline phases was carried out using the diffraction pattern files of the JCPDS (International Center for Diffraction Data).

The densification rate (or relative density) of the sintered samples was calculated by the relation between the density value determined by Archimedes' method and the theoretical density obtained by helium pycnometer (AccuPyc 1330 V2.04N) on powdered samples ( $<63\ \mu\text{m}$ ) of the sintered composite.

The fracture surface of sintered samples was characterized by field emission scanning electron microscopy (FESEM, Quanta FEG 650, Thermo Fisher Scientific, USA) in the backscatter electron mode.

Thermal (specific heat, diffusivity, and conductivity), electrical (conductivity) and mechanical (Young's modulus and flexural strength) properties of the composite were determined on the sintered composites. All the properties were measured in the in-plane direction of samples, except thermal properties. These were measured in the through-plane direction and the value in the in-plane direction was indirectly calculated by means of the Wiedemann–Franz law with a modified Lorenz number [28–30], where a value of the electrical conductivity in the through-plane  $<0.1\ \text{MS/m}$  ( $0.08\ \text{MS/m}$ ) was assumed [24,26,27]. The thickness of the samples (3 mm) does not allow measuring the other properties in the through-plane direction because this thickness was not sufficient to machine specimens. Anyway, properties are worse in through-plane direction because of graphite lamellae disposition on the specimen favorably oriented in the in-plane direction [24,26,27], as it was checked by scanning electron microscope.

Regarding mechanical properties, Young's modulus was measured using resonance frequency equipment (Grindosonic MK7, Belgium). The flexural strength of the sintered samples was determined by three-point bending tests [C1161 – 13. Standard Test Method for Flexural Strength of Advanced Ceramics at Ambient Temperature] in specimens of  $3\ \text{mm} \times 4\ \text{mm} \times 40\ \text{mm}$  using a universal mechanical testing machine (Shimadzu-series AGS-IX, Japan) with a 10 kN load cell at a crosshead speed of  $0.5\ \text{mm}\ \text{min}^{-1}$ . The flexural strength ( $\sigma$ ) was calculated using Eq. 1:

$$\sigma = \frac{3FL}{2wt^2} \quad (\text{Eq. 1})$$

where  $F$  is the load (force) at the fracture point,  $L$  is the length of the support span,  $w$  and  $t$  are the width and the thickness of the sample, respectively.

Electrical conductivity was determined on the sintered sample in the in-plane direction using Sigma Scope SMP350 from Helmut Fischer GMBH equipment. 10 measurements were made on each surface of the sintered sample and the mean value of the 20 measurements was considered as representative of the electrical conductivity of the composite.

Thermal conductivity is an indirect measurement calculated in the through-plane direction from the thermal diffusivity and the specific heat using Eq. 2:

$$\lambda = \alpha \cdot \rho \cdot c_p \quad (\text{Eq. 2})$$

where  $\lambda$  is the thermal conductivity ( $\text{W/mK}$ ),  $\alpha$  is the thermal diffusivity ( $\text{mm}^2/\text{s}$ ),  $\rho$  is the density ( $\text{g/cm}^3$ ) and  $c_p$  is the specific heat ( $\text{J/gK}$ ). This way, thermal diffusivity was measured in the through-plane direction using LFA 457 MicroFlash Netzsch

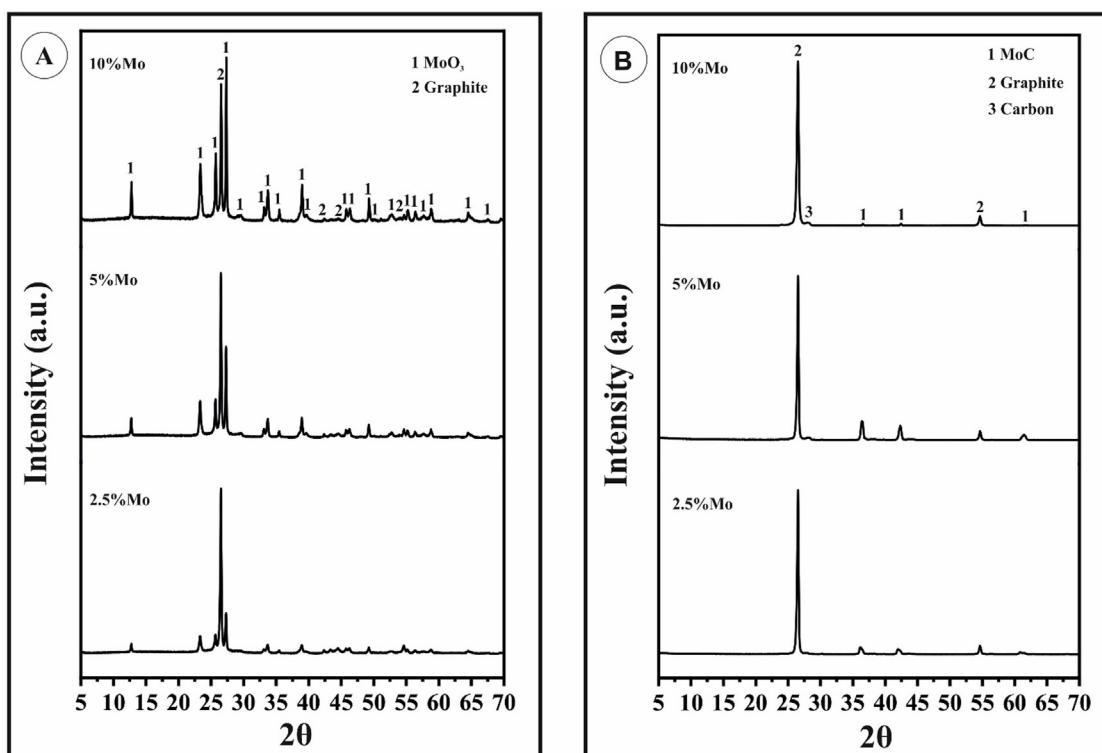


**Fig. 1** – X-ray diffraction patterns of: (A) powders obtained after heat treatment at 450 °C for 2 h in air; (B) samples sintered in spark plasma sintering apparatus.

equipment, which is based on the flash method, on squared specimens of 10 mm × 10 mm × 3 mm. On the other hand, specific heat was determined using a C80 (Setaram Instrumentation) calorimeter, equipped with stainless steel cells (S60/1413). Measurements were made in continuous mode: heating ramp of 0.1 °C min<sup>-1</sup> from 20 to 40 °C with 2 h of stabilization at the start and end temperatures. Data was processed with the Calisto Software. Thermal conductivity values in-plane were calculated using Eq. 3 considering the above-mentioned assumptions:

$$\frac{k}{\sigma} = LT \quad (\text{Eq. 3})$$

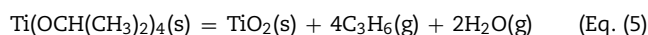
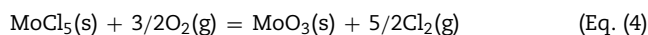
where  $k$  is the thermal conductivity,  $\sigma$  is the electrical conductivity,  $L$  is the modified Lorenz number and  $T$  is the temperature.

## Results and discussion

### Phase identification

Colloidal processing was employed, as mentioned, to obtain the composite because this technique ensures a more homogenous distribution of the second phases in the graphite matrix. The mixture of graphite with the precursors (MoCl<sub>5</sub> and Ti[OCH(CH<sub>3</sub>)<sub>2</sub>]<sub>4</sub>) was first heated at 120 °C for 24 h to start the nucleation of molybdenum and titanium and to evaporate the alcohol, but chemical transformations were not experienced at this stage. Afterward, dried powders

were subjected to heat treatment at 450 °C for 2 h in air to eliminate chloride and isopropoxide traces. This heat treatment involved the transformation of the precursors into oxides according to reactions 4 and 5 [31]:



The product of the chemical reaction (Eq. 4) was observed in X-ray diffraction analyses (that of titanium was not clearly observed due to both the quantity of titanium, but it formed during the sintering a complex carbide phase with the molybdenum, (Ti<sub>1-x</sub>,Mo<sub>x</sub>)<sub>1-y</sub>C<sub>y</sub>, which stabilized the cubic molybdenum carbide phase) see Fig. 1a. Peaks corresponding to molybdenum oxide (VI) (JCPDS: 01-089-7112) increase in intensity as the molybdenum content grows.

After reactive sintering, where oxides of molybdenum and titanium were reduced in the SPS machine, and transformed into carbides, independent of the molybdenum content, graphite (JCPDS: 00-056-0159) and MoC (JCPDS: 01-089-2868) are the main mineralogical phases (see Fig. 1b, corresponding to the sintered composites). MoC has cubic structure ( $a = 4.27 \text{ \AA}$ ), which corresponds to the carbide of molybdenum that, according to the Mo-C binary phase diagram, is formed at high temperature (which is stable at room temperature due to the presence of titanium, as it was already reported). Carbon donates electrons to the metal atoms and the coordination of metal atoms changes to form the carbide structures. The stability of this carbide structure is promoted by the

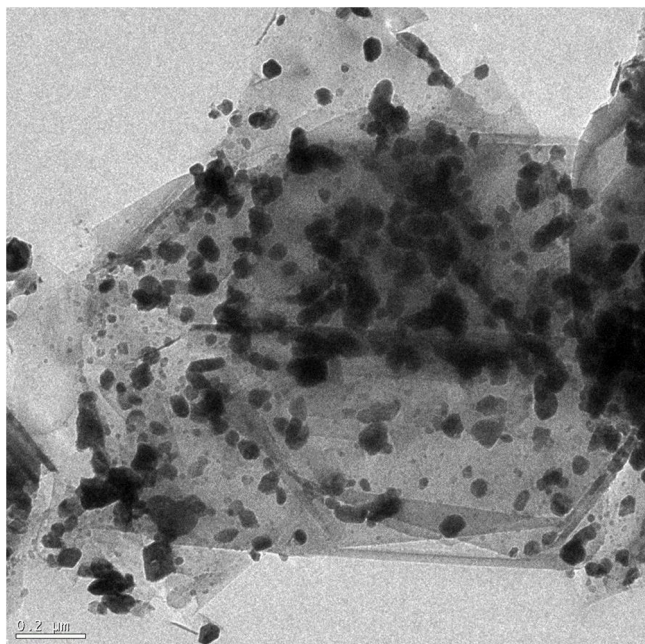


**Fig. 2 – HRTEM image of graphite–molybdenum composite synthesized by colloidal route (sample graphite–5 vol.% Mo in the image).**

covalent nature of the metal–carbon bond. The formation of the MoC starts at low temperature with the reaction of the molybdenum and graphite to form hexagonal or orthorhombic Mo<sub>2</sub>C. The process continues with the diffusion of carbon inside Mo<sub>2</sub>C to finally generate MoC. The stabilization of the α-MoC<sub>1-x</sub> at room temperature is promoted by small additions of titanium. Otherwise, this phase (cubic) results only stable at temperatures above 1960 °C according to the Mo–C binary phase diagram. Molybdenum carbides and, in particular MoC, are beneficial for the mechanical properties of the composite and the suitable distribution of carbides within the graphite matrix has also a great influence on them. Nevertheless, MoC at grain boundaries or in acicular form are detrimental for the strength of the composite [23,26,27].

#### Microstructural characterization

Fig. 2 shows a HRTEM image of the composite, graphite in light gray color and MoC in black color, with a globular shape and a particle size around 10–100 nm, appears adequately distributed in the graphite matrix constituent because

of the colloidal processing technique. There is chemical affinity between molybdenum and graphite [23], which can be also deduced from the X-ray diffraction analyses. Thus, hexagonal Mo<sub>2</sub>C will appear above 1000 °C as a consequence of the carbon atoms diffusion inside of the molybdenum bcc lattice interstitials. This results in the formation of hexagonal Mo<sub>2</sub>C when the amount of carbon reaches 33 at.%. Diffusion of carbon inside Mo<sub>2</sub>C continues and MoC is formed, which justifies the identification of MoC in the samples, as it was already pointed out.

Diffusion processes have relevant importance in the formation of carbides. Thus, carbon is a relatively small atom that can rapidly displace throughout metal carbide lattices via interstitial vacancies [32]. On the other hand, the opposite mechanism, displacement of metal atoms in graphitic materials, is comparatively slow and difficult [27].

Field Emission Scanning Electron Microscopy (FESEM) was employed to study the microstructure of the fracture surface of the sintered samples. Fig. 3 shows the microstructures of the sintered composites of graphite with 2.5 vol.%, 5 vol.% and 10 vol.% Mo (and 1 vol.% Ti). Several conclusions can be deduced from these figures. It is possible to see in all the cases that the second phase is homogeneously distributed in the matrix of graphite, which has later influence in the properties of the composite. For the greatest contents in molybdenum (10 vol.% Mo), the size of this phase, which sintered appears as MoC, ranges from hundreds of nanometers to several microns due to the agglomeration of the particles related to the Mo content. In the case of composites with 2.5 vol.% and 5 vol.% Mo, the size of the second phases does not exceed 1 μm.

Images of the surface of fracture were taken from samples broken by three-point bending test. Fig. 4 corresponds to the sample graphite–10 vol.% Mo–1 vol.% Ti. It is possible to see that graphite lamellae appear oriented perpendicular to the pressing direction, which confirms the anisotropic behavior of the composite. This results in better properties in the in-plane direction than in the through-plane direction, as it is going to be later demonstrated. This anisotropic behavior is a potential advantage in the directional dissipation of heat.

#### Density

Natural graphite powders are characterized by exhibiting self-lubricating properties that make possible to obtain green samples with high densification (~85%) using very low values of pressure, as high pressures involve risks of delamination of the green compacts. Anyway, the values of densification are far from those of other common ceramic materials, as silicon

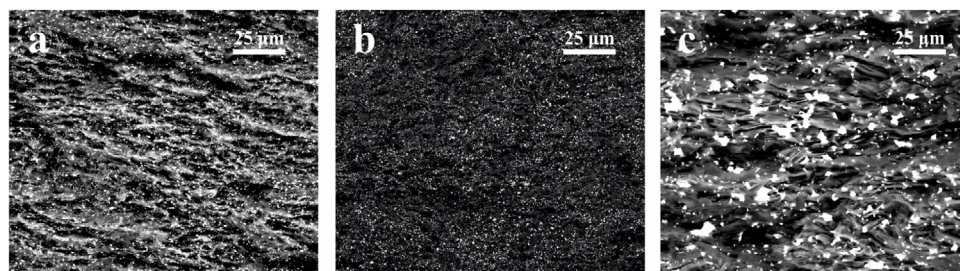


**Fig. 3 – FESEM images of doped graphite with (a) 2.5 vol.% Mo, (b) 5 vol.% Mo and (c) 10 vol.% Mo**

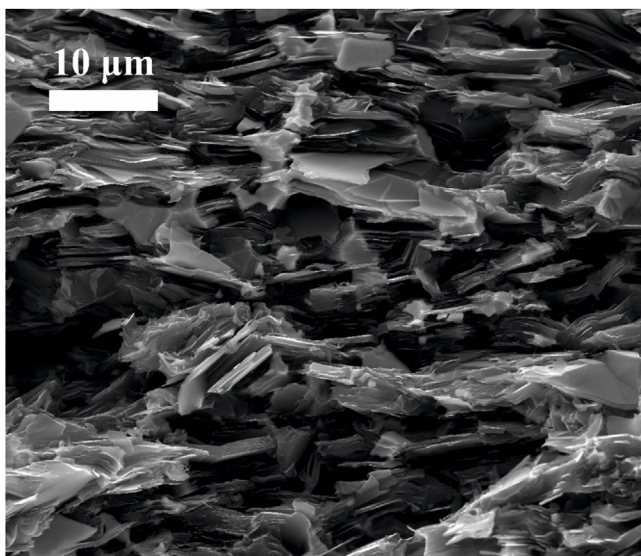


**Fig. 4 – SEM image corresponding to the surface of fracture of the sample graphite-10 vol.% Mo-1 vol.% Ti.**

carbide or alumina refractories, which even approach the theoretical density. In the case of graphite materials, according to Aguiar et al. [33], it is difficult to obtain densification rates >85% for non-conventional shapes, because of the high pressures required to obtain near-net shapes. In any case, values of densification do not exceed 95% even when greater pressures (to obtain green compacts) are used in other research works as in Suárez and coauthors [27]. In the case of the samples of this manuscript, the pressure applied to obtain green compacts was 15 MPa (uniaxial pressing) and values of densification rate are comparable for the three compositions ( $\approx 85\%$ ). This value of applied uniaxial pressure is 20 times smaller than that used by Guardia-Valenzuela and collaborators [24] and 3 times smaller than that employed by Suárez and colleagues [27]. Temperature is also important in the densification of the composite. The temperature at the dwell time was 2400 °C in this research, which is 200 °C lower than in the case of Guardia-Valenzuela et al. [24] and 400 °C greater than in the case of Suárez et al. [27]. In this second case, the higher temperature compensates at a certain extent the effect of the pressure applied to obtain the green compacts. Thus, these values of densification, see Table 1, are obtained, in general, without presence of liquid phase. Within this context, titanium melts at 1668 °C, which gives as result a small fraction of transitory liquid that will immediately react with the carbon

to form a titanium-molybdenum complex carbide. Moreover, a eutectic point at 2200 °C for  $\sim 3$  wt. % carbon is found in the Mo-C binary phase diagram, which might locally have resulted in liquid phase at the sintering temperatures in zones locally enriched in molybdenum. Undoubtedly, this small fraction of liquid phase might have promoted the transport of mass and, therefore, the sintering of the composite.

#### Mechanical characterization

The Young's modulus and the flexural strength have been evaluated and the results can be found in Tables 2 and 3, respectively. The properties of molybdenum carbide-doped graphite show a clear anisotropic behavior since the properties depend on the orientation of the graphite flakes (see Fig. 4). Stronger interatomic bond appears in the perpendicular direction to the applied pressure. The presence of MoC nanoparticles, finely and homogeneously distributed, together with the strong carbide-graphite bond in samples obtained by colloidal route allows obtaining better mechanical properties in these composites than in the case of those obtained by simply mixing of powders [26].

#### Electrical conductivity

Electrical conductivity measurements on sintered samples are shown in Table 4. It is possible to see that increasing the molybdenum content represents a clear improvement of the electrical conductivity of the samples, particularly when the molybdenum content is as high as 10 vol.%. Therefore, electrical conductivity for this composite is 7.8 and 5.1 times greater than in the cases of 2.5 vol.% Mo and 5.0 vol.% Mo, respectively. This value is higher than that measured by Guardia-Valenzuela and colleagues [24] and Suárez and co-researchers [26,27] for composites of the graphite-molybdenum-titanium system with less molybdenum content.

#### Thermal conductivity

Values of the thermal conductivity in the graphite - molybdenum - titanium composite are shown in Table 5. These follow a similar trend to that of the electric conductivity, being higher in the in-plane than in the through-plane direction, with the greatest values for the composite with 10 vol.% Mo. This result, which is the same that in the case of the other properties, indicates that sintering graphite-molybdenum carbide-titanium carbide composites at temperatures significantly lower (2400 °C) than those proposed by Guardia-Valenzuela et al. [24] (2600 °C) is possible, as it was suggested by Suárez et al.

**Table 1 – Density of SPS sintered samples at 2400 °C for different molybdenum contents.**

Mo content (vol.%)	2.5	5.0	10.0
Green density (g/cm <sup>3</sup> )	2.08 ± 0.02	2.33 ± 0.03	2.50 ± 0.02
SPS sample density (%)	82.32	86.05	85.24

**Table 2 – Young's modulus of SPS sintered samples at 2400 °C for different molybdenum contents (in-plane).**

Mo content (vol.%)	2.5	5.0	10.0
Young's modulus (GPa)	113.93 ± 22.29	203.59 ± 32.87	224.19 ± 65.93

**Table 3 – Flexural strength of SPS sintered samples at 2400 °C for different molybdenum contents (in-plane).**

Mo content (vol.%)	2.5	5.0	10.0
Flexural strength (MPa)	36.13 ± 7.98	44.90 ± 3.56	53.45 ± 8.27

**Table 4 – Electrical conductivity of SPS sintered samples at 2400 °C for different molybdenum contents (in-plane).**

Mo content (vol.%)	2.5	5.0	10.0
Electrical conductivity (MS/m)	0.14 ± 0.02	0.21 ± 0.03	1.07 ± 0.04

**Table 5 – Thermal conductivity of SPS sintered samples at 2400 °C for different molybdenum contents.**

Mo content (vol.%)	2.5	5.0	10.0
Thermal conductivity (W/m °C) (through-plane)	10.26 ± 1.33	30.65 ± 3.54	19.04 ± 1.45
Thermal conductivity (W/m °C) (in-plane)	14.17 ± 2.25	79.76 ± 6.20	255.35 ± 44.01

**Table 6 – Relative values of the properties of the composites sintered at 2400 °C for different molybdenum contents (this indicates the number of times the parameter is greater in the case of the samples with 10 vol.% Mo).**

Mo content (vol.%)	2.5	5.0
Flexural strength (MPa)	1.5	1.2
Electrical conductivity (MS/m)	7.8	5.1
Thermal conductivity (W/m °C)	18.0	3.2

[26,27] Values of thermal conductivity obtained for 10 vol.% Mo are, comparatively with those indicated in Guardia-Valenzuela et al. [24], lower but sufficient for not as extremely demanding applications as colliders but for less demanding applications of light heat dissipation devices. These last devices habitually demand excellent thermal conductivity, lightness, thermal resistance, or machinability, among other properties, and aluminum or copper are typically used in this application. However, graphite–molybdenum composites are, comparatively with the copper and aluminum, lighter (<2.50 g/cm<sup>3</sup> of graphite–Mo–Ti composite, in front of the 2.7 g/cm<sup>3</sup> of the aluminum or 8.96 g/cm<sup>3</sup> of the copper), with comparable thermal conductivity (>255 W/m K of graphite–Mo–Ti composite, in front of the 220 W/m K of the aluminum or 400 W/m K of the copper), better machinability or resistance at higher temperatures. Within this line, using hard sintering conditions as high temperatures (exceeding 2600 °C as in Guardia-Valenzuela et al. [24]) or pressures (300 MPa as in Guardia-Valenzuela et al. [24]) involve more expensive equipment and greater consumption of energy resources, resulting in more expensive components.

## Discussion

Graphite–molybdenum–titanium composites were prepared by colloidal synthesis and sintered by Spark Plasma Sintering (SPS). It was possible to check that increasing the molybdenum content has had a noticeable influence on the properties of the composite (Table 6).

It is particularly relevant the influence of the molybdenum content on the electrical conductivity (and therefore on the thermal conductivity, since both parameters are related by the modified Wiedemann–Franz law). It is possible to see that increasing the metallic content, apart from improving the

mechanical properties of the composite, results in greater conductivities. Typical value of electrical conductivity of graphite in the basal plane is 3–5 × 10<sup>5</sup> S/m (special quality graphite can reach values of electrical conductivity as high as 2.4 MS/m, for example, the thermal pyrolytic graphite [24]). On the other hand, some metal carbides show electrical conductivities as that of the metal [34]. This question, apart from the fact that some metal carbides inhibit basal planes slip through a pinning effect, which improves mechanical properties, makes reactive metals (carbides) interesting to improve the thermal–electrical properties of graphite. Within this context, metallic molybdenum shows values of electrical conductivity as high as 20 MS/m, and high thermal conductivity too (around 140 W/m K). These high values result in the great values of electrical and thermal conductivities of the composite, when sintered together graphite and molybdenum (transformed into carbide during the sintering), which makes it interesting for thermal management applications.

Molybdenum carbide should be adequately distributed within the graphite matrix. With this regard, Suárez et al. [26] have already demonstrated the influence of the colloidal processing technique on the properties of graphite–molybdenum–titanium composite. Colloidal processing is a suitable manner to obtain better mechanical properties than in the simple mechanic mixing of the constituents, precisely due to the more homogeneous distribution of the second phase [26]. However, if the influence of the molybdenum content is added, it is possible to see that values of electrical and thermal conductivities further improve. In the case of the first property, it is close to 1.1 MS/m in the in-plane direction (for 10 vol.% Mo), which is similar to that obtained by Guardia-Valenzuela et al. [24] (for 4.5 vol.% Mo), although using a SPS temperature 200 °C lower in the research presented in this manuscript. Additionally, the value of pressure required to obtain the green compacts is significantly lower, 15 MPa, which is 20 times lower than that used by Guardia-Valenzuela et al. [24] (300 MPa). The temperature compensates the influence of the pressure required to obtain the green compacts in terms of improvement of the properties. This way, better properties than in Suárez et al. [27], where the best were obtained for 60 MPa of uniaxial pressure to obtain green compacts (and SPS temperature at dwell time of 2000 °C), are obtained when using pressure of 15 MPa to obtain the green compacts if the temperature is

increased up to 2400 °C. Thus, electrical conductivity is a 25% greater.

If the electrical conductivity is considered (and, therefore, the thermal conductivity), the composites obtained by colloidal synthesis and spark plasma sintering could be competitive in heat dissipation applications. They are, probably, not competitive with those proposed by Guardia-Valenzuela et al. [24] for extreme conditions applications of the Large Hadron Collider at CERN installations, but they might be applied in less demanding applications, i.e. heat dissipation, as it was already reported. In the case indicated in the manuscript, the temperature is 200 °C lower and the pressure required to obtain the green compacts is 20 times lower. Therefore, composites might be easily scaled up and used in less demanding thermal management applications.

## Conclusions

Graphite–molybdenum carbide–titanium carbide composites were manufactured by spark plasma sintering from powders prepared by colloidal route. The influence of the molybdenum content (2.5, 5.0 and 10.0 vol.%) was studied on green compacts at 2400 °C. Molybdenum content has a significant influence on the electrical and thermal properties, as well as on mechanical properties. This way, the composite with 10.0 vol.% Mo content exhibits mechanical, electrical, and thermal properties 1.5, 7.8 and 18 times greater than those of the composite with 2.5 vol.% Mo and, 1.2, 5.1 and 3.2 times greater than those of the composite with 5.0 vol.% Mo. Within this context, it is possible to obtain graphite–10 vol.% Mo composites, using pressures to obtain green compacts 20 times lower than other researchers and sintering temperatures 200 °C lower. Therefore, graphite–molybdenum carbide–titanium carbide composites might be produced under less severe conditions of processing to be used in thermal management applications.

## Authors' contribution

**Conceptualization:** A. Fernández, R. Torrecillas; **Data curation:** Marta Suárez, Daniel Fernández-González, Juan Piñuela-Noval; **Formal analysis:** Marta Suárez, Daniel Fernández-González, Juan Piñuela-Noval, José Serafín Moya; **Funding acquisition:** A. Fernández, R. Torrecillas, Daniel Fernández-González, Juan Piñuela-Noval; **Investigation:** Marta Suárez, Daniel Fernández-González, Juan Piñuela-Noval, Luis Antonio Díaz, Amparo Borrell; **Methodology:** Marta Suárez, Daniel Fernández-González, Juan Piñuela-Noval; **Project administration:** A. Fernández, R. Torrecillas; **Resources:** Marta Suárez, Daniel Fernández-González; **Supervision:** A. Fernández, R. Torrecillas; **Validation:** Marta Suárez, Daniel Fernández-González, Juan Piñuela-Noval; **Visualization:** Marta Suárez, Luis Antonio Díaz, Amparo Borrell; **Roles/Writing – original draft:** Marta Suárez, Daniel Fernández-González; **Writing – review & editing:** Marta Suárez, Daniel Fernández-González, Juan Piñuela-Noval, José Serafín Moya.

## Acknowledgements

This research was funded by the Spanish Ministry of Science and Innovation. Call Programa Estatal de I+D+i Orientada a los Retos de la Sociedad (RTI2018-102269-BI00).

Daniel Fernández-González acknowledges the grant (Juan de la Cierva-Formación program) FJC2019-041139-I funded by MCIN/AEI/ 10.13039/501100011033 (Ministerio de Ciencia e Innovación, Agencia Estatal de Investigación).

Amparo Borrell acknowledges for her RYC-2016-20915.

Juan Piñuela Noval acknowledges the Programa “Severo Ochoa” of Grants for Research and Teaching of the Principality of Asturias for the funds received for the elaboration of the Ph.D. Thesis (Ref: BP20 041).

Authors are grateful to Ainhoa Macías San Miguel from Nanomaterials and Nanotechnology Research Center (CINN) for providing excellent technical assistance.

## REFERENCES

- [1] M. Humenik, D.W. Hall, R.V. Alsten, Graphite-base cermets: a new material for bearing, electrical and high-temperature applications, *Met. Progr.* 81 (1962) 101–108.
- [2] J. White, R. Price, Hot-working of graphite for graphite-matrix nuclear fuels, *Carbon* 2 (1965) 327–330, [http://dx.doi.org/10.1016/0008-6223\(65\)90001-1](http://dx.doi.org/10.1016/0008-6223(65)90001-1).
- [3] R. Staffler, G. Kneringer, E. Kny, N. Reheis, Metal/graphite-composites in fusion engineering, in: *IEEE Thirteenth Symposium on Fusion Engineering*, Knoxville, TN, USA, 1989, pp. 955–958.
- [4] D. John, G.M. Jenkins, Hot-working and strengthening in metal carbide-graphite composites, *J. Mater. Sci.* 21 (1986) 2941–2958, <http://dx.doi.org/10.1007/BF00551515>.
- [5] T. Etter, J. Kuebler, T. Frey, P. Schulz, J.F. Löffler, P.J. Uggowitzer, Strength and fracture toughness of interpenetrating graphite/aluminium composites produced by the indirect squeeze casting process, *Mater. Sci. Eng. A* 386 (2004) 61–67, <http://dx.doi.org/10.1016/j.msea.2004.06.066>.
- [6] J.K. Chen, I.S. Huang, Thermal properties of aluminum–graphite composites by powder metallurgy, *Compos. Part B-Eng.* 44 (2013) 698–703, <http://dx.doi.org/10.1016/j.compositesb.2012.01.083>.
- [7] T. Etter, P. Schulz, M. Weber, J. Metz, M. Wimmeler, J.F. Löffler, P.J. Uggowitzer, Aluminium carbide formation in interpenetrating graphite/aluminium composites, *Mater. Sci. Eng. A* 448 (2007) 1–6, <http://dx.doi.org/10.1016/j.msea.2006.11.088>.
- [8] V. Oddone, B. Boerner, S. Reich, Composites of aluminum alloy and magnesium alloy with graphite showing low thermal expansion and high specific thermal conductivity, *Sci. Technol. Adv. Mat.* 18 (2017) 180–186, <http://dx.doi.org/10.1080/14686996.2017.1286222>.
- [9] M. Byun, D. Kim, K. Sung, J. Jung, Y.S. Song, S. Park, I. Son, Characterization of copper–graphite composites fabricated via electrochemical deposition and spark plasma sintering, *Appl. Sci.-Basel* 9 (2019) 2853, <http://dx.doi.org/10.3390/app9142853>.
- [10] M.M. Dewidar, J.K. Lim, Manufacturing processes and properties of copper–graphite composites produced by high frequency induction heating sintering, *J. Compos. Mater.* 41 (2007) 2183–2194, <http://dx.doi.org/10.1177/0021998307074145>.



- [11] J. Kovacik, S. Emmer, Cross property connection between the electric and the thermal conductivities of copper graphite composites, *Int. J. Eng. Sci.* 144 (2019) 103130, <http://dx.doi.org/10.1016/j.ijengsci.2019.103130>.
- [12] J. Liu, K. Sun, L. Zeng, J. Wang, X.P. Xiao, J. Liu, C.J. Guo, Y. Ding, Microstructure and properties of copper-graphite composites fabricated by spark plasma sintering based on two-step mixing, *Metals* 10 (2020) 1506, <http://dx.doi.org/10.3390/met10111506>.
- [13] A. Mazloum, J. Kovacik, S. Emmer, I. Sevostianov, Copper-graphite composites: thermal expansion, thermal and electrical conductivities, and cross-property connections, *J. Mater. Sci.* 51 (2016) 7977–7990.
- [14] A. Mazloum, J. Kovacik, A. Zagrai, I. Sevostianov, Copper-graphite composite: shear modulus, electrical resistivity, and cross-property connections, *Int. J. Eng. Sci.* 149 (2020) 103232, <http://dx.doi.org/10.1007/s10853-016-0067-5>.
- [15] F. Nazeer, Z. Ma, L. Gao, F. Wang, M.A. Khan, A. Malik, Thermal and mechanical properties of copper-graphite and copper-reduced graphene oxide composites, *Compos. Part B-Eng.* 163 (2019) 77–85, <http://dx.doi.org/10.1016/j.compositesb.2018.11.004>.
- [16] Z. Xiao, R. Chen, X. Zhu, Z. Li, G. Xu, Y. Jia, Y. Zhang, Microstructure, and physical and mechanical properties of copper-graphite composites obtained by in situ reaction method, *J. Mater. Eng. Perform.* 29 (2020) 1696–1705, <http://dx.doi.org/10.1007/s11665-020-04646-8>.
- [17] J. White, J. Pontelandolfo, Graphite-carbide materials prepared by hot-working with the carbide phase in the liquid state, *Nature* 209 (1966) 1018–1019, <http://dx.doi.org/10.1038/2091018a0>.
- [18] J. White, J. Pontelandolfo, Graphite-carbide materials prepared by hot-working with a dispersed liquid-carbide phase, *Carbon* 4 (1966) 305–314, [http://dx.doi.org/10.1016/0008-6223\(66\)90043-1](http://dx.doi.org/10.1016/0008-6223(66)90043-1).
- [19] J. White, J. Pontelandolfo, HWLC graphites prepared by hot-working extruded stock, *Carbon* 6 (1968) 1–2, [http://dx.doi.org/10.1016/0008-6223\(68\)90043-2](http://dx.doi.org/10.1016/0008-6223(68)90043-2).
- [20] Y. Harada, G.A. Rubin, Fabrication and characterization of metal carbide-graphite composites, in: Presented at the 68th Annual Meeting of The American Ceramic Society, May 9, Washington, D.C., 1966.
- [21] R. Matthews, Deformation and Strengthening in Molybdenum Carbide – Natural Graphite Composite Materials (Ph.D. thesis), University of Wales, 1970.
- [22] N. Mariani, Development of Novel, Advanced Molybdenum-based Composites for High Energy Physics Applications (Ph.D. Thesis), Milan Polytechnic, 2014.
- [23] A. Bertarelli, S. Bizzaro, A molybdenum carbide/carbon composite and manufacturing method, *Int. Pat. Appl.* (2016), PCT/EP2013/072818.
- [24] J. Guardia-Valenzuela, A. Bertarelli, F. Carra, N. Mariani, S. Bizzaro, R. Arenal, Development and properties of high thermal conductivity molybdenum carbide – graphite composites, *Carbon* 135 (2018) 72–84, <http://dx.doi.org/10.1016/j.carbon.2018.04.010>.
- [25] K. Huang, K.C. Bi, C.S. Liang, S. Lin, W.J. Wang, T.Z. Yang, J. Liu, R. Zhang, D.Y. Fan, WangYG, M. Lei, Graphite carbon-supported Mo<sub>2</sub>C nanocomposites by a single-step solid state reaction for electrochemical oxygen reduction, *PLOS ONE* 18 (2015) 1–11, <http://dx.doi.org/10.1371/journal.pone.0138330>.
- [26] M. Suárez, D. Fernández-González, L.A. Díaz, A. Borrell, J.S. Moya, A. Fernández, Synthesis and processing of improved graphite-molybdenum-titanium composites by colloidal route and spark plasma sintering, *Ceram. Int.* 47 (2021) 30993–30998, <http://dx.doi.org/10.1016/j.ceramint.2021.07.267>.
- [27] M. Suárez, D. Fernández-González, D.F. Gutiérrez-González, L.A. Díaz, A. Borrell, J.S. Moya, R. Torrecillas, A. Fernández, Effect of green body density on the properties of graphite-molybdenum-titanium composite sintered by spark plasma sintering, *J. Eur. Ceram. Soc.* 42 (2022) 2048–2052, <http://dx.doi.org/10.1016/j.jeurceramsoc.2021.12.073>.
- [28] B. Schultrich, W. Poßnecker, Thermal conductivity of cemented carbides, *J. Therm. Anal.* 33 (1988) 305–310, <http://dx.doi.org/10.1007/bf01914616>.
- [29] R.W. Powell, F.H. Schofield, The thermal and electrical conductivities of carbon and graphite to high temperatures, *Proc. Phys. Soc.* 51 (1939) 153–172, <http://dx.doi.org/10.1088/0959-5309/51/1/317>.
- [30] J. Kováčik, S. Emmer, J. Bielek, Cross-property connections for copper-graphite composites, *Acta Mech.* 227 (2016) 105–112, <http://dx.doi.org/10.1007/s00707-015-1411-6>.
- [31] P. Buerger, D. Nurkowski, J. Akroyda, M. Kraft, A kinetic mechanism for the thermal decomposition of titanium tetraisopropoxide, *Proc. Combust. Inst.* 36 (2017) 1019–1027, <http://dx.doi.org/10.1016/j.proci.2016.08.062>.
- [32] R.B. Matthews, G.M. Jenkins, The high temperature interaction between molybdenum and graphite, *J. Mater. Sci.* 10 (1975) 1976–1990, <http://dx.doi.org/10.1007/BF00754489>.
- [33] J.A. Aguiar, S. Kwon, B.D. Coryell, E. Eyeran, A.A. Bokov, R.H.R. Castro, D. Burns, H.T. Hartmann, E.P. Luther, Densification of graphite under high pressure and moderate temperature, *Mater. Today Commun.* 22 (2020) 100821, <http://dx.doi.org/10.1016/j.mtcomm.2019.100821>.
- [34] E. Parthe, V. Sadagopan, The structure of dimolybdenum carbide by neutron diffraction technique, *Acta Crystallogr.* 16 (1963) 202–205, <http://dx.doi.org/10.1107/S0365110X63000487>.